15èmes JOURNÉES DE L'HYDRODYNAMIQUE
22 - 24 novembre 2016 - Brest

New model of solid blocks in interaction for waves generation by landslides

Un nouveau modèle de blocs solides en interaction pour la génération de vagues par des glissements de terrain

Lucie Clous (1), **Stéphane Abadie** (1)
(1) Laboratoire SIAME, Université de Pau et des Pays de l'Adour

Abstract : A new model to simulate the interaction of several solid blocks with a free surface is presented in this paper. To this end, a Navier-Stokes model is extended to deal with solid/solid interaction. This is done by modelling the solid with penalised fluid (fluid with a high viscosity). The main issue is the coalescence of two rigid bodies when a collision occurs. To avoid this behaviour, a subroutine is implemented in the code that detects the collisions, computes the new motions for the rigid bodies, avoids the collision while applying the new motions on a short period of time by adding a volume force into the colliding discs. A first validation for two discs has been made and show that though the motions close to the collision do not exactly comply with the laws for solid mechanics, they are restored right after. Moreover, simulations with three fluids and several discs point the potential of this method for waves generated by landslides model as several rigid blocs.

Résumé : Un nouveau modèle pour simuler les interactions de plusieurs blocs solides avec une surface libre est présenté dans ce papier. Pour cela, un modèle Navier-Stokes est étendu pour gérer les interactions solide/solide. Cela est réalisé en modélisant le solide par un fluide pénalisé (fluide avec une viscosité élevée). Le problème principal est la coalescence de deux corps rigides quand ils entrent en collision. Pour éviter ce comportement, une subroutine est implémentée dans le code qui détecte les collisions, calcule les mouvements des corps rigides, évite la collision en appliquant les nouveaux mouvements sur un court laps de temps en ajoutant une force volumique sur les disques en collision. Une première validation pour deux disques a été faite et montre que même si les mouvements proches de la collision ne respectent pas exactement les lois de la mécanique des solides, ils sont restaurés juste après. De plus, des simulations avec trois fluides et plusieurs disques montre le potentiel de la méthode pour les vagues générées par des glissements de terrain modélisés par plusieurs blocs rigides.

1 Introduction

Tsunamis can be generated by subaerial landslides as the falling of a flank of a volcano, pyroclastic flow or rockslides in mountain natural reservoir. Some examples of subaerial landslides that have generated a tsunami are Lituya Bay, Alaska in 1958 [5], Aisen, Chile in 2007 [15], [17], Tafjord, Norway in 1934 [8]. For the tsunami generated by a pyroclastic flow, it is difficult to have recent data, a famous case is the Krakatau eruption in 1883 [3].

To make numerical simulations of the wave generation by a landslide, approximations have to be done. The main choices are on the slide model and the flow model. The possible flow models vary from shallow water equations (Harbitz [9]), to Navier-Stokes (Heinrich [10], Abadie [2], [1]), including Boussinesq equations (Lynett and Liu [13], Watts et al. [21]) and fully nonlinear potential flow theory (Grilli and Watts [7]). Considering the slide rheology, some have considered one rigid block (Heinrich [10], Abadie [2] Figure 1b), or a fluid (Abadie et al. [1] Figure 1a, Viroulet [19]). However, these landslide models do not take into account the interactions between the several solid blocks composing the slide in reality. Recently, to get round this, simulations with a coupled CFD-DEM model have been carried out for waves generation by the slide of granular medium (Shan and Zhao [18], Zhao [22]).

In the present work, a landslide model composed of multi-blocks is considered (Figure 1c). A penalty method has already been employed by [2] for a single block model in a Navier-Stokes code. In this paper, a multi-block approach is presented allowing to take into account block/block and block/water interactions. This model is based on a mix of a penalty model to rigidify fluid portions and additional volume forces ([4]) to mimic contact forces. Compared to last attempts to simulate waves generated by granular medium based on the DEM method, the present approach allows a direct simulation of the interaction of the blocks with the free surface which is not possible so far in DEM. But the counterpart is the heavier resolution required around the blocks. In this paper we present the basis of the model and preliminary validation results.

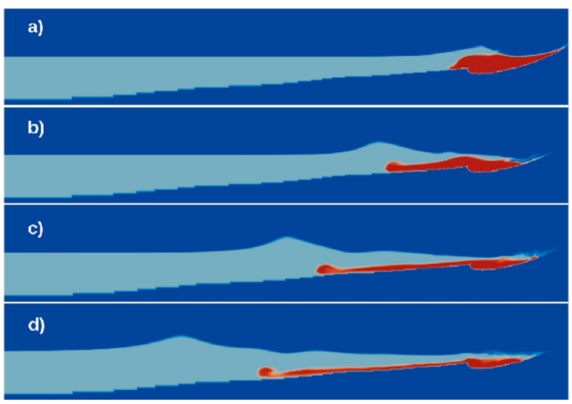

(a) 2D computations on Cumbre Vieja Volcano, La Palma, Canary Island, [1]

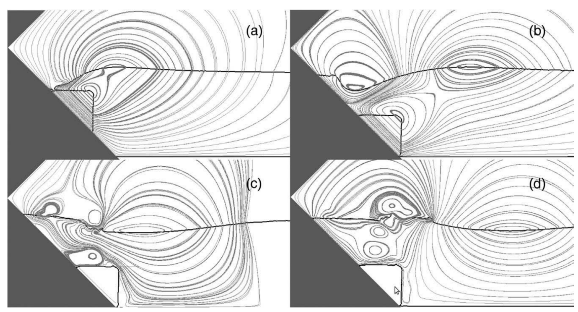

(b) Computations of triangular block sliding down an incline, [2]

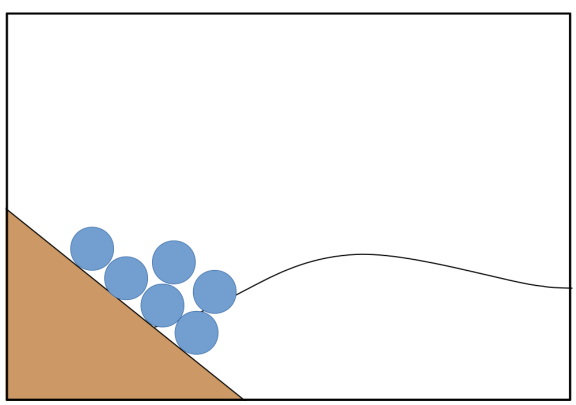

(c) New model of several solid discs of penalised fluid in interaction sliding into water

Figure 1 – Three models of landslides: fluid, one solid block, several solid blocks

2 Method

2.1 Model presentation

2.1.1 Governing equations

The simulation of waves generated by landslide is a problem composed of two fluid phases (air and water) and solid bodies. Whereas the fluid flow is governed by the Navier-Stokes (NS) equations (1), the solid motions are obtained by the Newton's law. Here, by employing a penalty method, only the NS equations will be solved for fluid flow and fluid/solid interactions.

The code that is used is Thetis, a numerical simulation tool developed by the I2M Laboratory in Bordeaux. It enables to resolve various problems: fluid flows, thermal transfers or porous media. The approach is Eulerian with a fixed mesh. In this paper, only the incompressible NS equations for Newtonian fluids are presented:

$$\begin{cases} \nabla \cdot v = 0 \\ \rho \left(\dfrac{\partial v}{\partial t} + (v \cdot \nabla) v \right) + \nabla p - \nabla \cdot [\mu (\nabla v + \nabla^t v)] = \rho b \end{cases} \tag{1}$$

2.1.2 Solving Navier-Stokes equations

Temporal discretization The Euler scheme of order 1 is used:

$$\frac{\partial v}{\partial t} = \frac{v^{n+1} - v^n}{\Delta t^n} \tag{2}$$

Apply to the Navier-Stokes equations (1), it leads to the following system.

$$\begin{cases} \nabla \cdot v^{n+1} = 0 \\ \rho^n (\dfrac{v^{n+1}}{\Delta t^n} + (v^{n+1} \cdot \nabla) v^{n+1}) + \nabla p^{n+1} - \nabla \cdot [\mu^n (\nabla v^{n+1} + \nabla^t v^{n+1})] - \rho^n b = \rho^n \dfrac{v^n}{\Delta t^n} \end{cases} \tag{3}$$

To give a linear formulation of the problem, the convective term $(v^{n+1} \cdot \nabla) v^{n+1}$ is linearised as $(v^n \cdot \nabla) v^{n+1}$.

Velocity-pressure decoupling The velocity-pressure decoupling is realised by the Augmented Lagrangian method. The pressure term is made explicit and the problem is reformulated. The new problem consists of optimizing the search of the saddle point associated to le Augmented Lagrangian. The method is iterative, the system is:

$$\begin{cases} \rho^n (\frac{v^{n,k+1}}{\Delta t^n} + (v^{n,k} \nabla) v^{n,k+1}) - \rho^n \mathbf{b} - \nabla p^{n,k} - \nabla [\mu^n (\nabla v^{n,k+1} + \nabla^t v^{n,k+1})] \\ -r_u \nabla (\nabla . v^{n,k+1}) = \rho^n \frac{v^n}{\Delta t^n} \\ p^{n,k+1} = p^{n,k} - r_p \nabla \cdot v^{n,k+1} \end{cases} \tag{4}$$

with k the method iteration and n the temporal iteration
and r_u and r_p two strictly positive convergence parameters

The algorithm convergence is reached when $(v^{n,k+1}, p^{n,k+1}) = (v^{n,k}, p^{n,k})$. The advantage of this method is the explicit computation of the pressure where no limit conditions on its value is required.

Spatial discretization The spatial discretization is realised by the finite volume method. The terms of the equations are expressed by a conservative form in order to use the Stokes formula on the control volume (V_Ω):

$$\frac{1}{V_\Omega} \int_\Omega (\nabla . F) \, dv = \frac{1}{V_\Omega} \int_\Gamma F.\mathbf{n} \, ds \tag{5}$$

$$\text{with} \quad \int_\Gamma F.\mathbf{n} \, ds = \int_{\Gamma_N} F.\mathbf{n}_N \, ds + \int_{\Gamma_S} F.\mathbf{n}_S \, ds + \int_{\Gamma_E} F.\mathbf{n}_E \, ds + \int_{\Gamma_O} F.\mathbf{n}_O \, ds \tag{6}$$

F is the considered variable, Δ_i the interface of the volume V_Ω with the neighbour volume oriented along i and n_i the normal to the interface Δ_i.

Moreover, the mesh is shifted and is composed of several grids: a main grids for scalar parameters, a grid for each velocity component, a viscosity grid.

2.1.3 VOF method

Once the pressure and velocity fields are computed, the interfaces between fluids have to be determined. The method that is used is the Volume Of Fluid (VOF) method. The interface is represented by a volume fraction of one of the two fluid in each cell. The variable is the colour function defined on each control volume as:

$$\begin{cases} \Phi_{F_i} = 1 \quad \text{if the fluid } F_i \text{ occupies all the control volume} \\ \Phi_{F_i} = 0 \quad \text{if the fluid } F_i \text{ is not present in the control volume} \\ 0 < \Phi_{F_i} < 1 \quad \text{if the fluid } F_i \text{ occupies partially the control volume} \end{cases} \tag{7}$$

The evolution of the interface is represented by the iso-contour of the colour function $\Phi_i = 0.5$.

The VOF-PLIC method employed here consists of a construction of the interface by segments of straight line. It is composed of three steps:

1. computation of the interface position from the Φ_i values
2. interface transportation according to the velocity field
3. computation of new values of the colour functions in the domain

2.1.4 Penalty method

The modelling of a solid based on the Navier-Stokes equations (8) can be achieved by annulling the local deformation. This can be obtained by imposing the dynamic viscosity tend to infinity, this way the only solution is for the local deformation term $\nabla v + \nabla^t v$ to be null. As in the numerical code, it is not possible to impose in infinite value, the viscosity is fixed to a very high value determined by a criterion on the overall deformation of the penalised fluid set by Ducassou et al. [4]. This way the fluid/solid interaction is computed implicitly by the Navier-Stokes model.

$$\rho \left(\frac{\partial v}{\partial t} + (v \cdot \nabla) v \right) + \nabla p - \nabla \cdot [\mu(\nabla v + \nabla^t v)] = \rho b \tag{8}$$

Collision between two rigid bodies The penalty method described here-before enables to solve the fluid/solid interaction in a NS code. Nevertheless in case of solid/solid interaction, the behaviour observed, which is due to the large viscosity value in rigid area, is a perfectly plastic collision where the two bodies coalesce after the crash. This is not the behaviour expected by the collision of two rigid bodies during a landslide. Additional volume forces are imposed on penalized area to hinder the contact and therefore the coalescence. These volume forces are calculated so that blocks trajectory approaches the one which would have been generated by the real contact. For this purpose a subroutine in implemented in the NS code that aims to:

- Detect the neighbour rigid bodies
- Detect the possible collision with neighbours and compute the occurring crash time
- Compute and apply the new motion of the rigid body after a collision

As already said, the change of motions of the rigid bodies is realised by applying a volume force on the penalised fluid, namely changing the term b in the NS equations. This change is active only over a short period of time (less than 5 time steps) and only in case of collision between rigid bodies.

2.2 Collision detection and velocity change

2.2.1 Detection of collision

As a first approach, the geometry of rigid bodies is only disc in 2D simulation. In the remainder of this paper, the rigid bodies are referred as discs.

Neighbour detection Several algorithms already exist for neighbour search, see [16], [14]. As in CFD, equations are solved on a grid, this same grid is used for neighbour cell detection named as conventional cell model in [14]. On this grid, the presence of disc is known at each node in an array. This array is later referred to as the identification array. Unlike the array containing the colour that gives only the presence of a certain phase, the identification array hold the presence of a specific solid by a number that specifies the disc present. Knowing this, two solutions are considered:

1. Detection of neighbours using an array. For each point of the pressure grid, if this point belongs to a disc, its neighbour cells are tested for the presence of another disc. These tests are performed by reading the value in the identification array. The size of the neighbour zone can be adjusted by controlling the number of cells tested in all directions.

   For instance, on the Figure 2, the size of the zone is one cell in each direction. One neighbour cell tested around the point P, belonging to the disc number 2, detects the presence of the disc number 1.

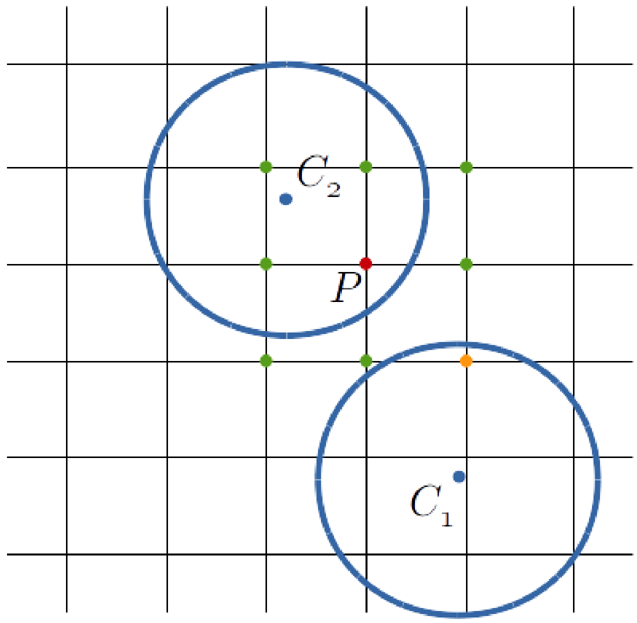

Figure 2 – Neighbour disc detection using the identification array: one neighbour detected at the orange point

2. Detection of neighbours using the distance to the centre. With this approach, the size of the detection zone is independent of the cell size. This zone is an annulus of centre, the centre C of the disk, interior radius R and exterior radius $R+\delta$. For each point of the pressure grid, the distance to the disc centres is computed, if this value is below $R+\delta$ for a disc i, the value in the identification array is read. If this value is different from i or 0 (no disc present), then this disc is considered as a neighbour of the disc i.

   For instance, on the Figure 3, the disc 1 is considered a neighbour of the disc 2 because the point P is at a distance lower than $R+\delta$ from C_1 and belongs to the disc 2.

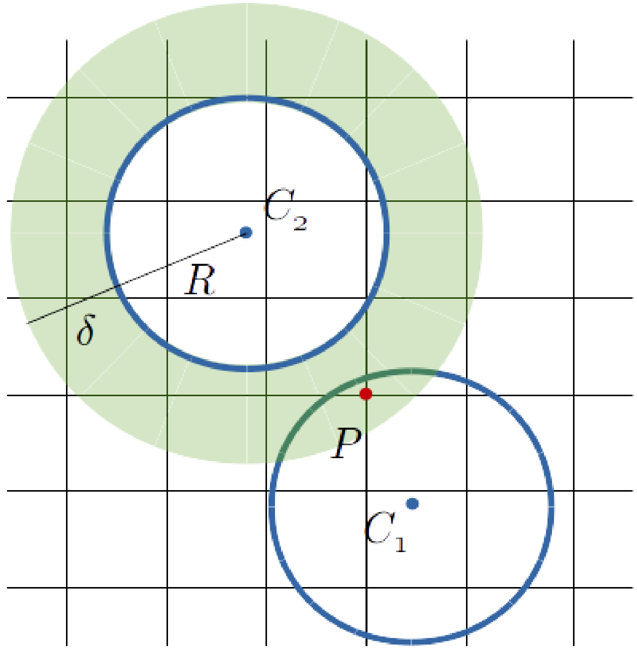

Figure 3 – Neighbour disc detection using the distance to the centre

Collision test After the detection of the neighbours, the next question is to know if they are likely to collide. A subroutine is developed to test the collision of two neighbours, and if positive, the time and distance to the collision.

The distance vector between the two centres is as follows:

$$\overrightarrow{d} = \overrightarrow{X_2}(0) - \overrightarrow{X_1}(0) + (\overrightarrow{V_2} + \overrightarrow{V_1})t \tag{9}$$

The two discs collide if the distance between the centres is the sum of the two radii, namely if $\overrightarrow{d} \cdot \overrightarrow{d} = (r_1 + r_2)^2$. Using the equation (9), we get a quadratic equation to solve :

$$at^2 + 2bt + c = 0 \tag{10}$$

$$\text{with} \quad a = (V_{1x} - V_{2x})^2 + (V_{1y} + V_{2y})^2$$
$$b = (X_{2x} - X_{1x})(V_{2x} - V_{1x}) + (X_{2y} - X_{1y})(V_{2y} - V_{1y})$$
$$c = (X_{2x} - X_{1x})^2 + (X_{2y} - X_{2y})^2 - (r_1 + r_2)^2$$

The reduced discriminant $\Delta = b^2 - ac$ is calculated. Depending on its value, several cases are distinguished:

- $\Delta < 0$: no real solution, no collision
- $\Delta \geq 0$: one or two real solutions: $t_1 = \frac{-b-\sqrt{\Delta}}{a}$ and $t_2 = \frac{-b+\sqrt{\Delta}}{a}$
  - if $t_1 < 0$ and/or $t_2 < 0$: no collision
  - if $t_1 > 0$ and $t_2 > 0$: collision at time $t_c = min(t_1, t_2)$

2.2.2 Computation of the velocity after collision

The collision is supposed without friction and with a Newton coefficient of restitution that can vary the behaviour between perfectly inelastic to perfectly elastic collision.

Collision between two discs After calculating the time of collision, the velocity of both discs after the impact V_1^+ and V_2^+ have to be determined, namely 4 unknowns.

Momentum conservation The momentum is conserved in the system composed by both discs, it leads to two equations:

$$m_1(\overrightarrow{V_1^+} - \overrightarrow{V_1^-}) = \overrightarrow{p_{12}} \tag{11}$$

$$m_2(\overrightarrow{V_2^+} - \overrightarrow{V_2^-}) = -\overrightarrow{p_{12}} \tag{12}$$

$$\text{with} \quad \overrightarrow{p_{12}} \quad \text{the exchanged momentum}$$

The sum of these equation leads to one vectorial equation, namely two scalar equations:

$$m_1\overrightarrow{V_1^+} + m_2\overrightarrow{V_2^+} = m_1\overrightarrow{V_1^-} + m_2\overrightarrow{V_2^-} \tag{13}$$

No friction As we consider no friction, the force is collinear to the normal of the contact point. It leads to the following scalar equation:

$$(\overrightarrow{V_1^+} - \overrightarrow{V_1^-}) \cdot \overrightarrow{T} = 0 \tag{14}$$

$$\text{with} \quad \overrightarrow{T} \quad \text{the tangent vector to the contact point}$$

Newton's restitution law There are two well-known coefficients of restitution, Poisson's and Newton's, [20]. As there is no friction in this model, the Newton coefficient of restitution is used. This leads to the last equation given by the Newton's restitution law:

$$(\overrightarrow{V_1^+} - \overrightarrow{V_2^+}) \cdot \overrightarrow{N} = -e(\overrightarrow{V_1^-} - \overrightarrow{V_2^-}) \cdot \overrightarrow{N} \tag{15}$$

$$\text{with} \quad e \quad \text{the restitution coefficient}$$

The coefficient of restitution e has its value between 0 and 1, with 1 for an elastic impact.

Solving the equation system The equation system is:

$$\left\{ \begin{array}{c} m_1V_{1x}^+ + m_2V_{2x}^+ = m_1V_{1x}^- + m_2V_{2x}^- \\ m_1V_{1y}^+ + m_2V_{2y}^+ = m_1V_{1y}^- + m_2V_{2y}^- \\ V_{1x}^+T_x + V_{1y}^+T_y = \overrightarrow{V_1^-} \cdot \overrightarrow{T} \\ V_{1x}^+N_x + V_{1y}^+N_y - V_{2x}^+N_x - V_{2y}^+N_y = -e(\overrightarrow{V_1^-} - \overrightarrow{V_2^-}) \cdot \overrightarrow{N} \end{array} \right. \tag{16}$$

This linear system can be written in a matrix way $AU = B$ with:

$$A = \begin{pmatrix} m_1 & 0 & m_2 & 0 \\ 0 & m_1 & 0 & m_2 \\ T_x & T_y & 0 & 0 \\ N_x & N_y & -N_x & -N_y \end{pmatrix} \tag{17}$$

$$U = \begin{pmatrix} V_{1x}^+ \\ V_{1y}^+ \\ V_{2x}^+ \\ V_{2y}^+ \end{pmatrix} \tag{18}$$

$$B = \begin{pmatrix} m_1V_{1x}^- + m_2V_{2x}^- \\ m_1V_{1y}^- + m_2V_{2y}^- \\ \overrightarrow{V_1^-} \cdot \overrightarrow{T} \\ -e(\overrightarrow{V_1^-} - \overrightarrow{V_2^-}) \cdot \overrightarrow{N} \end{pmatrix} \tag{19}$$

This system can easily be solved using a Gaussian elimination.

Collision between N_d discs The similar equations are written for the collision of a group of $N_d \geq 2$ discs.

$$\left\{ \begin{array}{l} m_iV_{ix}^+ - \sum\limits_{j \in P(i)} p_{i,jx} = m_iV_{ix}^- \\ m_iV_{iy}^+ - \sum\limits_{j \in P(i)} p_{i,jy} = m_iV_{iy}^- \\ p_{i,j}T_{i,jx} + p_{i,jy}T_{i,jy} = 0 \\ (V_{ix}^+ - V_{jx}^+)N_x + (V_{iy}^+ - V_{jy}^+)N_y = -e[(V_{ix}^- - V_{jx}^-)N_x + (V_{iy}^- - V_{jy}^-)N_y] \end{array} \right. \tag{20}$$

The first two equations are for each discs, namely N_d equations, the last two equations are for each pairs of discs in collision, namely N_p equations. This system of $N_d + N_p$ unknowns can also be solved with a Gaussian reduction.

Volume forces applied on a disc The volume force b that is applied on the disc of penalised fluid is as follows:

$$b = \frac{V_{target} - V_{current}}{\delta t} \tag{21}$$

A test on the disc velocity is done: the volume forces are applied on the disc until the error between the target value and the velocity value is less than 1%. This usually takes less than 5 time steps and in the worst cases, the force is stopped after 10 time steps.

3 Preliminary results

3.1 Validation for the collision between two discs

To assure the resolution of the velocities after the collision, simulations are performed with two discs. The positioning of the discs is shown on the Figure 4. The two discs have the same radius $R = 0.1\,m$. The disc D_1 is accelerated to a velocity $\overrightarrow{V_1} = V_1^- \overrightarrow{x}$ with $V_1^- = 1\,m.s^{-1}$, the velocity of the disc D_2 is null. The distance x is fixed for all computations to $0.5\,m$ and the distance y varies from 0 to $2R$. Velocities results after the collision computed by the subroutine and compared with the one computed with a python routine can be found on Figure 5. This python routine solves first the collision test discussed in the subsection 2.2 to determined the time of collision, and then solves the system of equation in case of collision between two discs the system of equation that gives velocities after the crash. The values are the same for almost all simulations, except some values for the disc D_1 around $y = 0.14\,m$ but the error is very small.

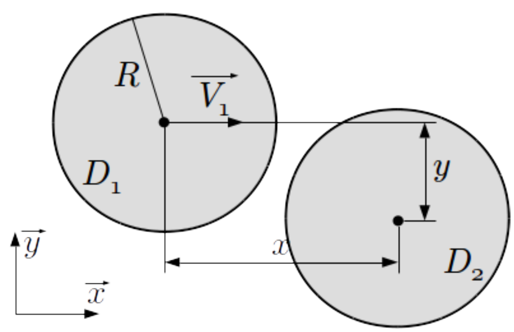

Figure 4 – Scheme of the simulation

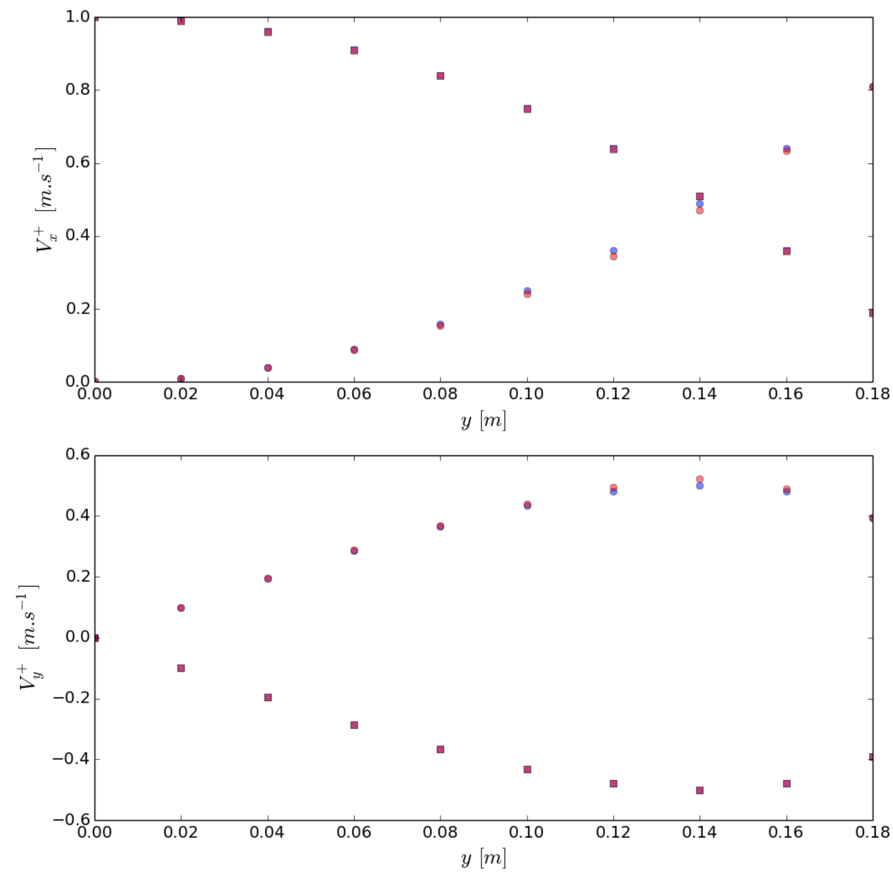

Figure 5 – Comparison of the velocities after the collision between the python routine and Thetis simulation. In blue: python results, in red: Thetis results; circle: disc D_1, square: disc D_2

Other validation cases are still ongoing. They encompass the validation of the drag around a cylinder at high Reynolds, the fall of a cylinder and the interaction with the free surface and other experiments involving a slide made up of several cylinders and generating a wave. The objective is to determine the required amount of cells to resolve satisfactorily the fluid/solid interaction.

3.2 Collision between several discs and water entry

The following results are just example of simulations without validations but they illustrate the long term objectives of this work.

Water entry One of the advantages of using the penalty method to model solid bodies is that the interactions with fluids are solved directly in the Navier-Stokes code. Simulations can be run with three fluids (air, water and penalised fluid). It has been possible to compute the fall of a rigid disc into a water reservoir after bouncing on the bottom boundary. The disc arrives into water with an oblique velocity and create a splash.

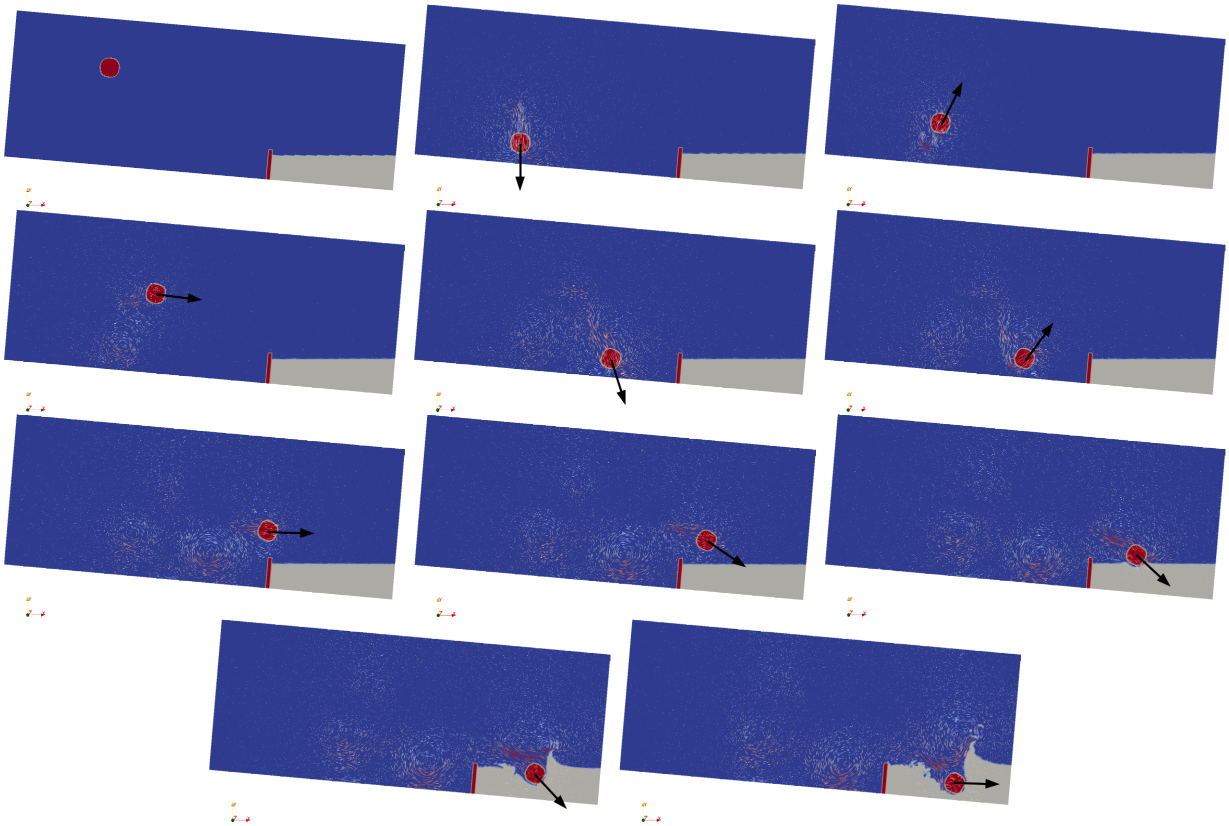

Figure 6 – Simulation of a disc of penalised fluid (red) falling into a water reservoir (grey), blue fluid is air, colour lines show the direction and amplitude of velocity of the fluids, the black arrow shows the direction of the disc velocity

Simulation with more than two discs To illustrate the collision between more than two discs, a simulations with 16 discs has been run. The subroutine managing the collisions is still in development. Although the following results have not been validated with experiment or another code, they show the potential of this method concerning the solid/solid interactions.

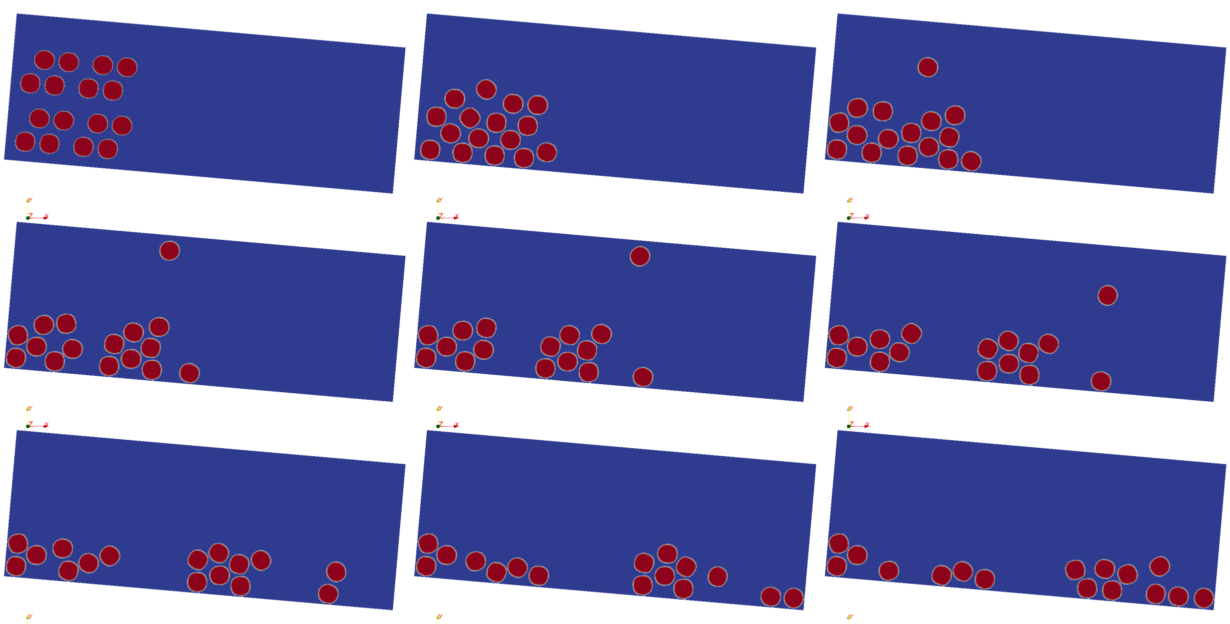

Figure 7 – Simulations of 16 discs of penalised fluid falling on a slope

With the possibility of three fluids simulations and multiple rigid bodies, computations of landslides composed of several solid blocs and sliding into water can be imagined. We are of course far from the resolution of the complex grain/grain interactions at all the scales and in 3D. But this approach can help simulate and better understand simple but relevant cases of academic multi-block slides in interaction with water. Furthermore, coupled with a macroscopic soil rheology such as $\mu(I)$ (GDR MiDi [6], Jop et al. [11], [12]) for instance, it can allows to simulate in a original way a real slide taking into account the interaction of the larger blocks explicitly with the penalty method while the finer soil portion would be modelled macroscopically.

4 Conclusions

This paper presented a new model of rigid bodies of penalised fluid in interaction for simulations of waves generated by landslides. It consists of a subroutine that manages the solid/solid interaction in a Navier-Stokes model with VOF interface tracking. By contrast with other work, the landslide is model as several rigid bodies and there is no external code to compute their motions. First validation simulations have been realised. The main conclusions are as follows:

- A first validation comparing to a python routine showed that the subroutine succeeds in detecting the collision, computing and applying the new motions after the crash.
- Thanks to this model, the solid blocks are able to interact with boundaries, fluids and other rigid bodies as simulations with several blocks and water reservoir pointed out.

The validation process is still in progress. To validate the effort on the rigid disc, a simulation of a high Reynolds flow around a fixed disc of penalised fluid is run. The value of drag coefficient and distribution of pressure can be compared with experimental data. Other validation cases will be run once experimental data are available like the fall of a cylinder into water and the sliding of several cylinders on an incline and into water. This validation cases aim to determined the minimum resolution of the mesh to ensure the satisfactory solving of the fluid/solid interaction.

Acknowledgement

This work was funded in part by the FP7 EU research program ASTARTE (Grant No.:603839).

References

[1] S. M. Abadie, J. C. Harris, S. T. Grilli, and R. Fabre. Numerical modeling of tsunami waves generated by the flank collapse of the Cumbre Vieja Volcano (La Palma, Canary Islands): Tsunami source and near field effects. *Journal of Geophysical Research*, 117(C5), May 2012.

[2] Stéphane Abadie, Denis Morichon, Stéphan Grilli, and Stéphane Glockner. Numerical simulation of waves generated by landslides using a multiple-fluid Navier–Stokes model. *Coastal Engineering*, 57(9):779–794, September 2010.

[3] S. Carey, H. Sigurdsson, C. Mandeville, and S. Bronto. Pyroclastic flows and surges over water: an example from the 1883 Krakatau eruption. *Bulletin of Volcanology*, 57(7):493–511, April 1996.

[4] Benoît Ducassou. *Modélisation de l'intéraction entre un fluide à surface libre et un solide rigide soumis à des efforts extérieurs par une méthode pénalisation*. Thèse de doctorat, Université de Pau et des Pays de l'Adour, France, 2016.

[5] Hermann M. Fritz, Fahad Mohammed, and Jeseon Yoo. Lituya Bay Landslide Impact Generated Mega-Tsunami 50th Anniversary. *Pure and Applied Geophysics*, 166(1-2):153–175, February 2009.

[6] GDR MiDi. On dense granular flows. *The European Physical Journal E*, 14(4):341–365, August 2004.

[7] Stéphan T. Grilli and Philip Watts. Tsunami Generation by Submarine Mass Failure. I: Modeling, Experimental Validation, and Sensitivity Analyses. *Journal of Waterway, Port, Coastal, and Ocean Engineering*, 131(6):283–297, November 2005.

[8] C. B. Harbitz, G. Pedersen, and B. Gjevik. Numerical Simulations of Large Water Waves due to Landslides. *Journal of Hydraulic Engineering*, 119(12):1325–1342, December 1993.

[9] C.B. Harbitz. Model simulations of tsunamis generated by the Storegga Slides. *Marine Geology*, 105(1-4):1–21, March 1992.

[10] P. Heinrich. Nonlinear Water Waves Generated by Submarine and Aerial Landslides. *Journal of Waterway, Port, Coastal, and Ocean Engineering*, 118(3):249–266, May 1992.

[11] Pierre Jop, YoëL Forterre, and Olivier Pouliquen. Crucial role of sidewalls in granular surface flows: consequences for the rheology. *Journal of Fluid Mechanics*, 541(-1):167, October 2005.

[12] Pierre Jop, Yoël Forterre, and Olivier Pouliquen. A constitutive law for dense granular flows. *Nature*, 441(7094):727–730, June 2006.

[13] P. Lynett and P. L. F. Liu. A numerical study of submarine-landslide-generated waves and run-up. *Proceedings of the Royal Society A: Mathematical, Physical and Engineering Sciences*, 458(2028):2885–2910, December 2002.

[14] Hiroshi Mio, Atsuko Shimosaka, Yoshiyuki Shirakawa, and Jusuke Hidaka. Cell optimization for fast contact detection in the discrete element method algorithm. *Advanced Powder Technology*, 18(4):441–453, 2007.

[15] José Antonio Naranjo, Manuel Arenas, Jorge Clavero, and Oscar Muñoz. Mass movement-induced tsunamis: main effects during the Patagonian Fjordland seismic crisis in Aisén (45°25'S), Chile. *Andean geology*, 36(1), January 2009.

[16] Eric Perkins and John R Williams. A fast contact detection algorithm insensitive to object sizes. *Engineering Computations*, 18(1/2):48–62, 2001.

[17] Sergio A. Sepúlveda, Alejandra Serey, Marisol Lara, Andrés Pavez, and Sofía Rebolledo. Landslides induced by the April 2007 Aysén Fjord earthquake, Chilean Patagonia. *Landslides*, 7(4):483–492, December 2010.

[18] Tong Shan and Jidong Zhao. A coupled CFD-DEM analysis of granular flow impacting on a water reservoir. *Acta Mechanica*, 225(8):2449–2470, August 2014.

[19] Sylvain Viroulet. *Simulations de tsunamis générés par glissements de terrains aériens*. Thèse de doctorat, Aix-Marseille Université, France, 2013.

[20] Yu Wang and Matthew T Mason. Two-dimensional rigid-body collisions with friction. *Journal of Applied Mechanics*, 59(3):635–642, 1992.

[21] P. Watts, S. T. Grilli, J. T. Kirby, G. J. Fryer, and D. R. Tappin. Landslide tsunami case studies using a Boussinesq model and a fully nonlinear tsunami generation model. *Natural Hazards and Earth System Science*, 3(5):391–402, 2003.

[22] T. Zhao, S. Utili, and G. B. Crosta. Rockslide and Impulse Wave Modelling in the Vajont Reservoir by DEM-CFD Analyses. *Rock Mechanics and Rock Engineering*, 49(6):2437–2456, June 2016.